JOURNAL OF CATALYSIS 33, 7–16 (1974)

Kinetics of Ethylene Hydrogenation Over a Supported Nickel Catalyst

HO-PENG KOH AND R. HUGHES

Department of Chemical Engineering, University of Salford, Salford, M5 4WT, England

Received May 7, 1973

The kinetics of hydrogenation of ethylene over a supported nickel/silica–alumina catalyst powder have been investigated using a differential flow reactor. It was found that appreciable temperature gradients occurred even when an extremely dilute catalyst was used and when conversions were less than 3%. Purification of the ethylene feed from oxygen impurities removed all poisoning effects. From the kinetic results, a mechanism involving reaction between adsorbed ethylene and gaseous hydrogen is proposed.

INTRODUCTION

The heterogeneous catalyzed hydrogenation of ethylene has been investigated extensively in the past. However, the actual kinetics of the process are still controversial and have been further complicated by the poisoning effects which are frequently encountered.

Most of the earlier work was carried out in closed systems, often on metal films, and the progress of the reaction followed by noting the change of system pressure with time. In recent years more attention has been devoted to flow systems using supported metal catalysts. A survey of the literature reveals that there is general agreement that the reaction is first order in hydrogen and the activation energy is low, ranging up to 14 kcal mole^{-1}. The order in ethylene is more controversial but where this has been determined a value of less than 0.4 is usually obtained. One unusual feature of the reaction is that the activation energy tends to decrease with rise in temperature and a negative value has been reported in some instances (*1*, *2*). The temperature at which this negative value first appears has been designated as the inversion temperature and this occurs at temperatures from 90° to about 200°C, the precise value depending on the pressure used (*1*).

Earlier studies suggested that the reaction proceeds through an associative adsorption of ethylene but opinions differ whether the subsequent reaction goes via a Langmuir-Hinshelwood mechanism with adsorbed hydrogen or by an Eley-Rideal reaction with gas-phase or Van der Waals' adsorbed hydrogen. Farkas and Farkas (*3*), on the basis of exchange experiments, suggested a reaction involving dissociatively adsorbed hydrogen and adsorbed ethylene. Horiuti and Polanyi (*4*) proposed that the reaction goes through a half-hydrogenated state. Later, Jenkins and Rideal (*5*) postulated a mechanism involving reaction between adsorbed hydrogen on the nickel surface and gaseous ethylene. The dissociative adsorption of ethylene with the formation of poisonous acetylenic residues on the active sites was suggested to account for the observed adverse effect of ethylene on the reaction rate.

Investigations with flow systems have received significantly less attention. Beeck (*6*) suggested that some ethylene molecules are adsorbed on that part of the surface not covered by acetylenic complexes and that the rate-controlling step is the reaction

between adsorbed ethylene and adsorbed hydrogen. A fast reaction between gaseous ethylene and adsorbed hydrogen also occurs. Using the exchange reaction with deuterium, Twigg (*7*) concluded that hydrogen is first dissociated into atoms on the surface through reaction with adsorbed ethylene. Hydrogenation occurs with the addition of another hydrogen atom. Recently, Pauls *et al.* (*8*) and Kostenblatt and Ziegler (*9*) carried out experiments using flow systems with nickel on alumina catalysts. Both sets of authors obtained a rate equation which suggested a reaction between adsorbed ethylene and gaseous hydrogen, but because of the poisoning effects obtained with ethylene, the results were interpreted in terms of the Jenkins–Rideal mechanism (*5*), in which hydrogen is adsorbed on dual sites and reacts with gaseous ethylene, but with no adsorption possible on that fraction of the surface occupied with ethylene or acetylenic complexes.

As part of a wider study in which the hydrogenation of ethylene was used as a model reaction to study the effects of transport limitations on catalytic reactions, it was found necessary to redetermine the kinetics of this reaction on a silica–alumina-supported nickel catalyst. Preliminary work showed that even when using very small amounts of diluted catalyst in a differential reactor at conversions of less than 3%, steep temperature profiles developed in the catalyst bed. Because of this, the axial temperature distribution was measured at several points in the bed using fine thermocouple wires and thus the conversions were obtained at known bed temperatures.

Experimental Method

Materials

Hydrogen of 99.9% purity was obtained from cylinders, deoxygenated with a Deoxo Unit and dried with silica gel before use. Ethylene (C.P. grade 99.2% purity) was freed from oxygen by passing over freshly reduced MnO_2 granules and dried with silica gel. Ethane (99.2%) was used without further purification for calibration of the gas chromatograph.

The catalyst was prepared by impregnation of the silica–25% alumina powder of average diameter 60 μm (kindly donated by J. Crosfield & Sons Ltd.) with nickel nitrate solution to give a material containing 5% by weight of nickel. This was calcined at 500°C for 24 hr and after cooling was diluted with seven times its weight of silica–alumina support to give a final nickel content of 0.525%. This dilution procedure was found to be superior to the use of fine glass beads which tended to sinter when the catalyst was reduced in hydrogen at 400°C before use.

Apparatus

The apparatus is shown schematically in Fig. 1 and consists of a gas purification section, a flow monitoring system, the glass differential flow reactor, and a gas chromatograph. Flow rates were controlled with "Flostat" controllers and measured with rotameters.

The reactor used is illustrated in Fig. 2 and was designed so that the whole assembly could be immersed in an oil bath.

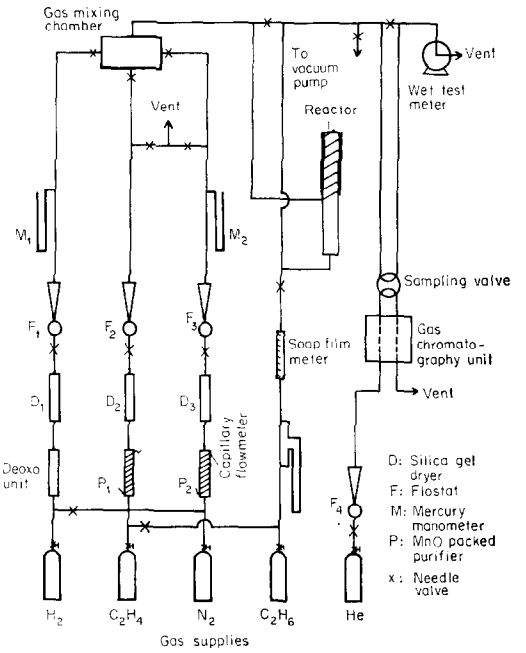

FIG. 1. Reactor flow system.

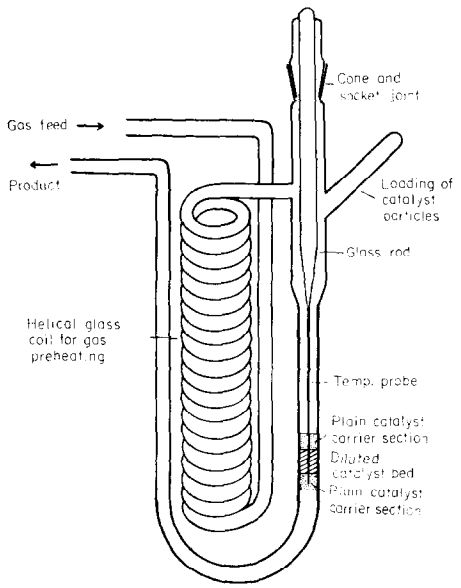

FIG. 2. Differential packed bed flow reactor for kinetic studies.

The mixed reactants were preheated in the coil and passed downward through the diluted catalyst bed of diameter 5.2 mm and length 7 mm, supported on either side by 5-mm sections of inert carrier. The temperature probe was constructed by attaching a multi-junction thermocouple of Pt–13% Rh/Pt wire, diameter 0.025 mm, to a thin glass rod of diameter 0.7 mm. The 4-junction thermocouple was secured to the glass rod by high temperature cement. The distance between junctions was measured using a travelling microscope and the probe was positioned centrally in the reactor so that after filling with catalyst the upper and lower thermocouple junctions just contained the bed of active material. In addition, a thermocouple junction was positioned outside the reactor tube level with the catalyst bed. Experiments in a wider bore reactor referred to later established that the radial temperature profile varied by about 3°C for temperature rises from 20° to 70°C over the central 40% of the bed diameter. Assuming that a similar profile was obtained in the smaller diameter reactor, the thermocouple probe could be positioned easily within this central region.

Procedure

After activating the MnO_2 by heating in hydrogen to 120°C the catalyst was reduced in hydrogen at 400°C for 25 hr using an electric furnace. The reactor was then removed from the furnace and positioned in the oil bath which had been adjusted to the required temperature. The gases were then admitted in the required ratio and temperatures and exit gas compositions recorded. Separation of hydrogen, ethylene, and ethane was achieved with the gas chromatograph using a 10-ft silica gel column at 55°C, with helium as carrier gas. The temperatures at the four junctions were measured in turn using a rotary selection switch and the temperatures recorded. The MnO_2 and catalyst were reduced between all experimental runs.

Calculation of Conversion and Average Bed Temperature

Because of the small amount of conversion (less than 3%) the reactor operates differentially. From the stoichiometry of the reaction, the mole fraction of ethane, N_C, is related to the conversion, X, by the expression,

$$X = N_C/(1 + N_C), \tag{1}$$

where X is defined as the fraction of ethylene in the total feed that is converted in the reactor containing a mass W of catalyst.

The reaction rate expressed in terms of the plug flow reactor equation is

$$R^* = F(dX/dW) \tag{2}$$

where F is the total gas feed rate. Therefore,

$$R^* = \frac{F}{(1 + N_C)^2}\frac{dN_C}{dW} \tag{3}$$

This expression can be integrated when operation is differential, using the arithmetic average of $1/(1 + N_C)^2$, i.e.,

$$R^* = F\frac{N_{Co}}{W}\left(\frac{1}{1 + N_C}\right)^2_{Av}, \tag{4}$$

where N_{Co} is the measured mole fraction of ethane in the product gas. The error in-

troduced by the use of this equation is less than 2% for ethane values up to 14% in the exit stream. In this work the ethane concentration was always less than 3% so the error is negligible.

The averaged reaction temperature inside the catalyst bed was obtained by the following procedure. From the reactor wall temperature and the axial temperatures a mean bed temperature was evaluated at each thermocouple position assuming a parabolic distribution of the radial profile. The arithmetic mean of these values was taken as the approximate temperature to correspond to the rate computed from Eq. (4). The corrrect temperature was evaluated by the following procedure. From the preliminary uncorrected results, a plot of reaction rate against temperature gave the rate as a function of radial and axial position in the bed. The total rate was then obtained by summing the individual rate contributions in the volumes at the known temperatures. This summed rate was equated to the experimental value of the rate to give the average temperature in the bed corresponding to the experimental rate.

Results and Discussion

The reaction experiments were carried out using hydrogen-rich gas mixtures containing 7 to 43% of ethylene. Because of the small particle size of the catalyst (average diameter 60 μm), mass and heat transfer resistances external to the particle were negligible. Most experiments were done using a gas flow rate of 3 cm^3 sec^{-1}, which corresponded to a space velocity of about 30 sec^{-1}. Initial reaction temperatures were in the range from 190°C down to room temperature but most of the results were obtained in the temperature range 90–190°C. Varying amounts of catalyst were used but the results reported refer to a fixed amount of the active catalyst (0.01 gm before dilution).

Preliminary experiments in a wider bore reactor in which 0.025 mm thermocouples were placed across the bed established that the radial temperature profiles were approximately parabolic. Very high temperatures were obtained in this reactor which in turn produced high conversions. All further experiments were made therefore in the smaller diameter reactor depicted in Fig. 2.

Blank experiments in which the reactor contained only catalyst support but with the thermocouples in position, established that no measurable conversion occurred under these conditions throughout the temperature range investigated.

Poisoning Effects

The catalytic reaction between hydrogen and ethylene is very susceptible to poisoning. Previous work has suggested (*5*) that the observed decline in rate with time is only partially attributable to gas phase impurities and the main cause of poisoning is dissociative adsorption of ethylene to give acetylenic complexes on the nickel surface. It has also been reported that the activity of the catalyst can be stabilized by pretreating the catalyst with a mixture of hydrogen and ethylene at relatively high reaction temperatures. This processing is believed to break down the acetylenic complexes into hydrogen and carbided residues and the rate of removal of these carbides by hydrogn is low at the subsequent (lower) temperatures employed for reaction.

In this work, preliminary experiments established that poisoning occurred both at high and low reactor temperatures and was severe for low temperatures. The catalyst pretreatment procedure, as advocated above, was employed but without much success. Thus, although catalyst pretreatment at the higher temperature of 160°C produced constant activity, no stable catalyst activity could be obtained at temperatures lower than this. In the present work the poisoning was thought to be caused by traces of oxygen present in the ethylene. In the original experimental procedure, any oxygen present in the ethylene was removed by passing the ethylene through MnO_2 granules which had been reduced in hydrogen at 250°C. Poisoning was present in experiments carried out immediately after this purification procedure. Adoption of a lower reduction temperature for the MnO_2

granules produced a more reactive MnO and in the subsequent experiments no poisoning effects were observed. At the reaction steady state, the activity of the catalyst remained constant for many hours during an experimental run and although most of the rates reported were obtained at temperatures above 90°C, reaction could still be observed at temperatures as low as 15°C. The use of a small amount of catalyst also enabled any poisoning effect to be readily detected.

Use of this purification procedure gave reproducible catalyst activity for all the series of runs in the low temperature region (up to about 140°C), but a gradual decrease in activity occurred in the higher reaction temperature region. This was observed even though the catalyst was reduced in hydrogen at 400°C between every series of runs. Inspection of the catalyst after several series of runs in this temperature region revealed that the catalyst bed now contained some black carbonaceous deposits. Similar deposits were also observed in the upstream catalyst carrier. On this basis, the gradual decline in catalyst activity at high reaction temperatures could not be attributed to dissociative adsorption of ethylene since the deposition was nonselective. Moreover, it has been demonstrated that if the surface is carbided, the catalyst activity is reduced for both high and low temperature regions, whereas the present results show that the catalyst activity at low temperatures was not affected. Deposition of carbon may be supposed to reduce slowly the number of active sites; this effect would be expected to be more important at higher temperatures where the availability of the surface becomes important because of the high reaction rate.

Observed Temperature Profiles

One of the major uncertainties in experimental kinetic studies of exothermic catalytic reactions is the actual temperature corresponding to the reaction rate measured. As indicated in the experimental section, isothermal behavior could not be obtained even when drastic dilution techniques to obtain lower conversion were adopted.

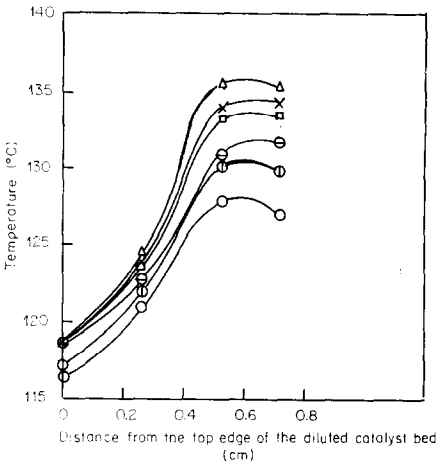

FIG. 3. Variation of axial temperature profiles in bed with mixture composition. Oil bath temp. = 115°C. Totaal gs flow rate = 3.3 cm^3 sec^{-1}. Mole % C_2H_4: ⊙ = 7.1, ⓘ = 11.2, × = 18.9, △ = 28.2, ⊡ = 34.7, ⊖ = 43.4.

The temperature distribution inside the catalyst bed was a function of the extent of conversion and the feed conditions and was measured during the reaction. Figures 3–5 show some typical longitudinal temperature distributions along the axis of the

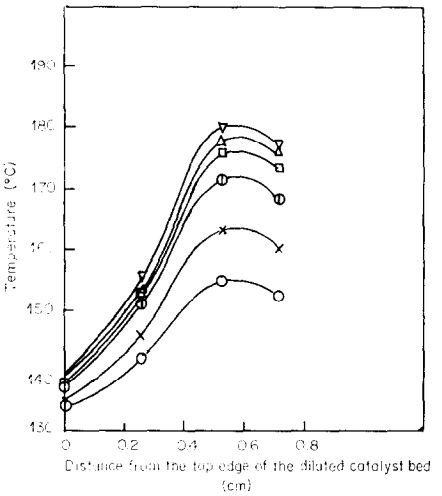

FIG. 4. Variation of axial temperature profiles in bed with mixture composition. Oil bath temp. = 134°C. Total gas flow rate = 3.1 cm^3 sec^{-1}. Mole % C_2H_4: ⊙ = 7.4, × = 12.2, ⓘ = 18.2, ⊡ = 24.1, ▽ = 29.6, △ = 37.3.

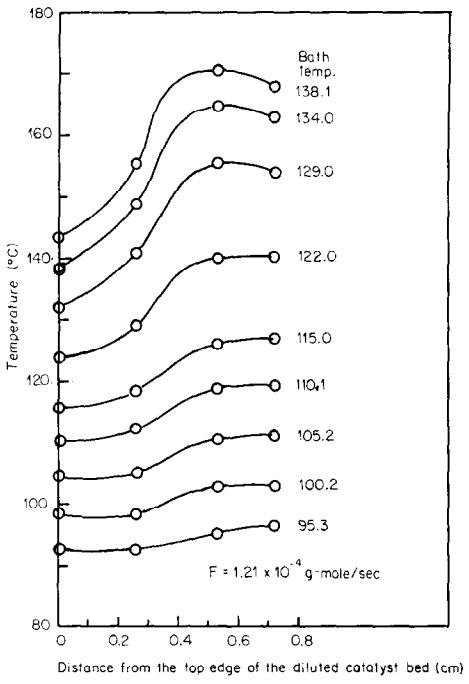

FIG. 5. Variation of axial temperature profiles with oil bath temperature. C_2H_4 conc.n = 31 mole %. Total gas flow rate = 3.0 cm³ sec⁻¹.

catalyst bed under steady-state conditions but for different operating conditions. Because of the small diameter of the catalyst bed, the radial temperature distribution within the bed was not measured but earlier experiments using a reactor of larger bore had established that the radial temperature distribution within the bed was approximately parabolic.

Figures 3 and 4 show the effect of mixture composition on the axial temperature profiles inside the catalyst bed at oil bath temperatures of 115° and 134°C, respectively. The temperature of the bed increased rapidly with bed depth and despite the use of a diluted catalyst, the maximum temperature rise was almost 40°C in some cases. In general, a slight decrease of temperature was found at the exit of the bed; this temperature decrease is caused by the external cooling. It will be noted that the maximum temperature rise in the bed does not occur when the concentration of ethylene is greatest. This is because, as explained later, the rate was found to be approximately first order in hydrogen and proportional only to a low fractional power of the ethylene concentration. Consequently the decrease in hydrogen concentration is in no way compensated by the increase in ethylene concentration and the reaction rate decreases, giving a corresponding lower temperature change in the bed.

Figure 5 shows the effect of the oil bath temperature on the axial temperature profiles at constant gas mixture composition. Clearly the temperature distribution inside the catalyst bed was reasonably uniform only at oil bath temperatures less than about 100°C.

Activation Energy

Experimental values of the activation energy measured for the reaction on the nickel catalyst reported in the literature vary from almost zero to 14 kcal mole⁻¹. The inconsistency of these results may be attributed to the difficulty in estimating the average temperature at which the reaction occurs. In the present studies, the value of the activation energy for the reaction was measured over a farily wide temperature range varying from 90° to 190°C. Arrhenius plots of the experimental data, as shown in Fig. 6, revealed a break occurring at about 135° to 150°C. The value of the activation energy obtained using a least squares method for the temperature between 90–135°C was 12.00 ± 0.95 kcal mole⁻¹, at a confidence level of 95%. In the high temperature region investigated (135–190°C), the activation energy decreased to a value of 6.4 ± 0.70 kcal mole⁻¹. The value of the activation energy measured in the low temperature region is in good agreement with other workers. However, a precise value for the activation energy at high reaction temperatures is not available to compare with present value of 6.4 kcal/gm mole. The change of slope of the Arrhenius plot has also been reported previously and an explanation (*10*, *11*) given on the basis of decreased adsorption of hydrogen or, alternatively, by postulating a competing reaction for ethylene at the higher reaction temperature. These features together with

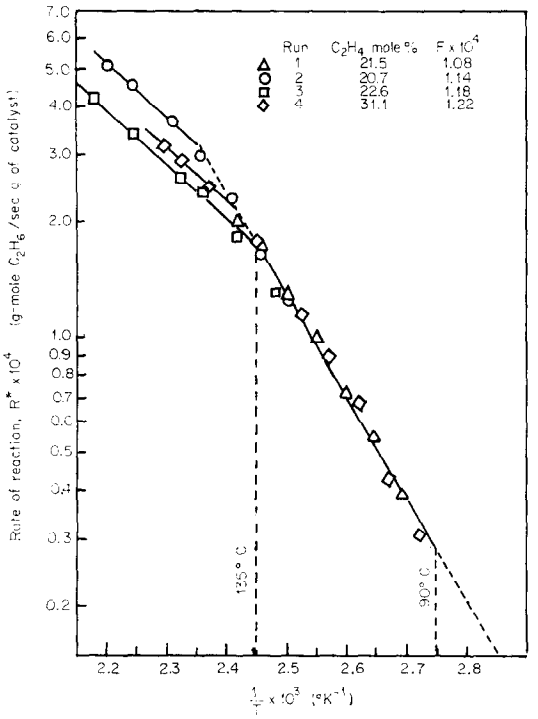

FIG. 6. Arrhenius plot of kinetic data.

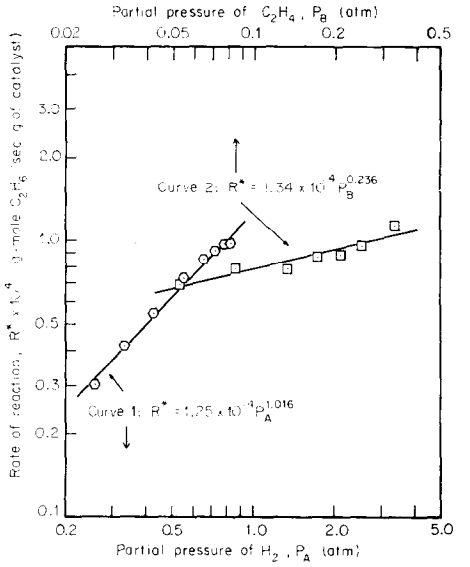

FIG. 7. Variation of reaction rate with partial pressures of ethylene and hydrogen. ⊙: $p_{C_2H_4}$ = 16.7%, $F = 0.83 \times 10^{-4}$, T_{av} = 120°C. ⊡: p_{H_2} = 67.0%, $F = 1.11 \times 10^{-4}$, T_{av} = 124°C.

the effect of ethylene concentration on the reaction rate at higher temperatures will be discussed later.

Rate Equation

The dependence of the reaction rate on the component partial pressures was studied at two temperature levels where the measured values of the activation energy were different. The earlier experimental procedure was planned to establish the effect of the average partial pressures of each component while holding the average partial pressures of the other component constant for a constant total gas flow rate. Nitrogen gas was employed as diluent to make up the total gas flow rate. Figure 7 shows the results obtained for the experiments with the concentrations of ethylene and hydrogen held constant in turn. Temperature corrections were applied in correlating the obtained data at an average value of the reaction temperature. The empirical dependences of the rate on the component partial pressures under two different reaction conditions were as follows:

$$R^* = 1.25 \times 10^{-4} P_A^{1.02} \quad \text{(at constant } P_B\text{, 120°C)} \quad (5)$$

$$R^* = 1.34 \times 10^{-4} P_B^{0.24} \quad \text{(at constant } P_A\text{, 124°C)}. \quad (6)$$

However, the use of this experimental procedure which kept one of the component partial pressures constant might presuppose advance knowledge of the exact effect of all the variables controlling the reaction rates. Hence, more experiments were carried out in which the partial pressures of the hydrogen and ethylene were varied while keeping only the total feed rate constant. Nitrogen was not used in these later experiments. The empirical dependence of the rate on the partial pressures obtained by a least squares method at two different temperature levels were as follows:

$$R^* = 2.93 \times 10^{-2} P_A^{1.09} P_B^{0.21} \quad (128°C) \quad (7)$$

$$R^* = 8.78 \times 10^{-4} P_A^{1.12} P_B^{0.36} \quad (162°C). \quad (8)$$

The first-order dependence on hydrogen

partial pressure is in agreement with the results reported above and also in agreement with the results of some of the earlier studies. Similar empirical dependence of the rate on the component partial pressures was observed over a nickel–alumina catalyst by Pauls *et al.* (*8*). The fractional order with respect to ethylene suggests a Langmuir type of mechanism with adsorption of ethylene on the surface.

The rate equation based upon the Langmuir adsorption theory and the equilibrium postulate can be derived by the assumption of a mechanism for the reaction and the supposition of a single rate-determining step in the process, the remaining steps occurring under equilibrium conditions. Within this framework the concept of the mechanism which best fits the kinetic data is adopted.

Many different mechanisms for the catalytic hydrogenation of ethylene may be formulated. The reaction may be supposed to occur by one of the following main routes: (1) Reaction between molecularly adsorbed hydrogen and adsorbed ethylene; (2) reaction between atomically adsorbed hydrogen and adsorbed ethylene; (3) reaction between ethylene in the gas phase and molecularly adsorbed hydrogen; (4) reaction between ethylene in the gas phase and atomically adsorbed hydrogen; or (5) reaction between hydrogen in the gas phase and adsorbed ethylene.

In principle the controlling step in each of these reaction processes may be adsorption of either hydrogen or ethylene, desorption of ethane, or surface reaction, modified where necessary because of the conditions of the mechanism postulated.

A systematic analysis for choosing the most plausible mechanism using the graphical method suggested by Sussman and Potter (*12*) was applied to all the mechanisms proposed. Since no ethane was used in the reactor feed and only a very small conversion was obtained, the ethane adsorption term could be considered negligible. The partial pressures of the remaining two components could be expressed in terms of either one. It is a requirement of the theory upon which these equations are based that the applicable equations should plot as a straight line with a positive intercept and a positive or negative slope, depending on the form of the equation.

Only three kinetic expressions were found to fit these conditions. These were for reaction between adsorbed ethylene and molecularly adsorbed hydrogen when desorption of ethane controls and for reaction between adsorbed ethylene and gaseous hydrogen when the rate-controlling step is either impact of hydrogen upon adsorbed ethylene or desorption of ethane. The appropriate equations are

$$\frac{p_A p_B}{R^*} = \frac{1}{\omega K_A K_B}(1 + K_A p_A + K_B p_B) = m + a p_A + b p_B \approx (m + a) + (b - a) p_B \quad (9)$$

$$\frac{p_A p_B}{R^*} = \frac{1}{\omega K_A}(1 + K_B p_B + K_C p_C) = m + b p_B + c p_C \approx m + b p_B \quad (10)$$

$$\frac{p_A p_B}{R^*} = \frac{1}{\omega K_B}(1 + K_B p_B) = m + b p_B, \quad (11)$$

where the final expressions preceded by the approximation sign refer to the conditions already assumed of negligible ethane concentration and therefore $p_C = 0$ and $p_A + p_B = 1$. In all these expressions the term ω contains the rate constant. The reaction between adsorbed hydrogen and adsorbed ethylene when ethane desorption controls, corresponding to Eq. (9), was rejected because of reports which have suggested that the amount of hydrogen adsorbed on the surface is very low (*7*, *13*). Equation (11), which gave a good fit, is based on the reaction between hydrogen in the gas phase and adsorbed ethylene when ethane absorption controls; it seems improbable because Rideal has shown (*1*, *5*) that the desorption of ethane was almost instantaneous and therefore could not be rate controlling. Therefore, although Eqs. (10) and (11) reduce to the same algebraic form when the amount of ethane is negligible, the mechanism best fitting the evidence is that of Eq. (10), based on ethylene adsorption with no adsorption of hydrogen or ethane and with the reaction between adsorbed

ethylene and gaseous hydrogen as the rate-controlling step. This equation is

$$R^* = \frac{kp_Ap_B}{1 + K_Bp_B} \qquad (12)$$

and a plot of the experimental results correlated with this expression is shown in Fig. 8.

The same rate equation has been proposed by other workers but used with different interpretations. Pauls *et al.* (*8*) and also Koestenblatt and Ziegler (*9*) put forward the reaction mechanism described above but abandoned it because of its inability to explain the poisoning effect of ethylene on the catalyst surface which they observed. The model of Jenkins and Rideal (*5*) was then employed to suggest the dissociative adsorption of ethylene with the formation of poisonous acetylenic complexes on the catalyst surface. However, the model was used with the assumption of negligible hydrogen adorption in order to obtain the above rate equation which best fitted their results.

In the present studies, however, no change in catalyst activity was detected and the proposed mechanism could then be applied directly. As shown in Fig. 8, Eq. (12) best fitted the kinetic data obtained at the two different temperature levels and use of the method of least squares gave the following numerical forms

$$R^* = \frac{5.73 \times 10^{-3}p_Ap_B}{1 + 22.67p_B} \text{ (at 128°C)} \qquad (13)$$

$$R^* = \frac{7.61 \times 10^{-3}p_Ap_B}{1 + 10.45p_B} \text{ (at 162°C).} \qquad (14)$$

In the above equations, the values of the ethylene adsorption equilibrium constant, K_B, were obtained as the quotients of the intercept and slope of the plots.

For a heterogeneous catalytic reaction, the complete rate expression describes not only the temperature variation of the rate constant but also the temperature variation of the orders of the reaction and of the adsorption coefficients. It is thus evident from the above rate expressions that the value of the ethylene adsorption equilibrium constant is lower at higher reaction temperatures. The decrease in K_B in the high reaction temperature region could explain the drop in the measured value of activation energy above 135°C. Generally, the heat of adsorption is a function of surface coverage, which may be due to surface heterogeneity or repulsion between molecules in the adsorbed layer. As a consequence, the temperature variation at constant reactant partial pressures affects not only coverage but also by extension the heat of adsorption. Thus, in the high re-

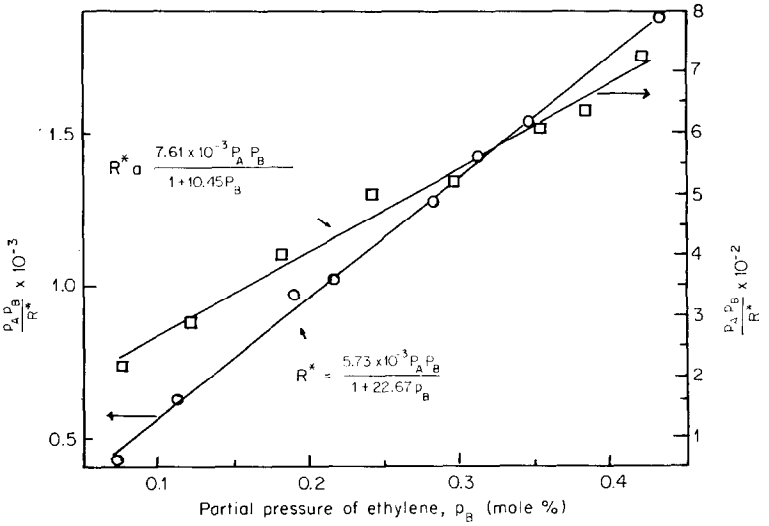

FIG. 8. Correlation of rate data. ⊙: $F = 1.32 \times 10^{-4}$, $T_{av} = 128$°C. ⊡: $F = 1.21 \times 10^{-4}$, $T_{av} = 162$°C.

action temperature region where the surface coverage is low, the apparent activation energy is lower than the true one by the heat of adsorption.

$$E_{obs} = E + \Delta H_a \qquad (15)$$

When the surface coverage is high at lower reaction temperatures, there is no desorption to allow for and hence the apparent activation energy is the true one. In the present case, the value of the activation energy decreased from 12.0 kcal/mole measured at lower temperatures, to 6.4 kcal/mole at higher temperatures.

For a general rate law of the form

$$R^* = (kp_Ap_B)/(1 + K_Bp_B), \qquad (16)$$

it follows that in the low temperature region $K_Bp_B \gg 1$, and the rate equation reduces to

$$R^* = kp_A. \qquad (17)$$

With the increasing temperature, ethylene coverage decreases, $K_Bp_B \ll 1$, and

$$R^* = kp_Ap_B. \qquad (18)$$

In the present work, the first-order reaction with respect to hydrogen at low temperature region has been confirmed experimentally. The Arrhenius plot (Fig. 6) shows that the concentration of ethylene has no significant effect on the rate measured in this temperature range. Limiting second-order behavior at high temperatures has also been detected since the rate is a slightly increasing function of ethylene concentration at temperature above 135°C. This tendency, however, was obscured to some extent because of the slight decline in catalyst activities encountered in the high temperature region. As shown in Fig. 6, run 2 with an ethylene concentration of 20.7 mole% should have a lower reaction rate than that obtained in run 3, which had a slightly higher ethylene concentration (22.6 mole%). Run 4 which was carried out after run 3 offset the decrease in catalyst activity because of its higher ethylene concentration and thus had a higher rate of reaction. The results showed that the level at which the reaction rate settled in the high temperature region was determined by the two balancing effects, i.e., the operating conditions of the catalyst and the value of the ethylene concentration.

References

1. Rideal, E. K., *J. Chem. Soc.* **121**, 309 (1922).
2. Kato, K., Takeuchi, N., and KuBota, H., *J. Chem. Eng. Japan* **2**, 204 (1969).
3. Farkas, A., and Farkas, L., *J. Amer. Chem. Soc.* **60**, 22 (1938).
4. Horiuti, J., and Polanyi, M., *Trans. Far. Soc.* **30**, 1164 (1934).
5. Jenkins, G. I., and Rideal, E. K., *J. Chem. Soc.* **2490**, 2496 (1955).
6. Beeck, O., *Disc. Far. Soc.* **8**, 118 (1950).
7. Twigg, G. H., *Disc. Far. Soc.* **8**, 152 (1950).
8. Pauls, A. C., Comings, E. W., and Smith, J. M., *Amer. Inst. Chem. Eng. J.* **5**, 453 (1959).
9. Kostenblatt, S., and Ziegler, E. N., *Amer. Inst. Chem. Eng. J.* **17**, 891 (1971).
10. Fulton, J. W., and Crosser, O. K., *Amer. Inst. Chem. Eng. J.* **11**, 513 (1965).
11. Sato, S., and Miyahara, K., *J. Res. Inst. Cat. Hokkaido Univ.* **13**, 10 (1965).
12. Sussman, M. V., and Potter, C., *Ind. Eng. Chem.* **46**, 457 (1954).
13. Twigg, G. H., and Rideal, E. K., *Proc. Roy. Soc.* **A171**, 55 (1939).